

Preferential interactions in pigmented, polymer blends – C.I. Pigment Blue 15:4 and C.I. Pigment Red 122 – as used in a poly(carbonate)–poly(butylene terephthalate) polymer blend

K.E. Fagelman, J.T. Guthrie*

Department of Colour and Polymer Chemistry, University of Leeds, Woodhouse Lane, Leeds, West Yorkshire LS2 9JT, UK

Received 12 November 2004; received in revised form 26 July 2005; accepted 1 August 2005

Available online 31 August 2005

Abstract

Some important characteristics of selected pigments have been evaluated, using the inverse gas chromatography (IGC) technique, that indicate the occurrence of preferential interactions in pigmented polymer blends. Attention has been given to copper phthalocyanine pigments and to quinacridone pigments incorporated in polycarbonate–poly(butylene terephthalate) blends. Selected supporting techniques were used to provide supplementary information concerning the pigments of interest, C.I. Pigment Blue 15:4 and C.I. Pigment Red 122. For C.I. Pigment Red 122 and for C.I. Pigment Blue, the dispersive component of the surface free energy decreases as the temperature increases, indicating the relative ease with which the molecules can be removed from the surface.

© 2005 Elsevier B.V. All rights reserved.

Keywords: Inverse gas chromatography; Pigment interactions; Polymer blends; Physical characterisation; Performance–composition relationships

1. Introduction

High-performance pigments are those with all-round properties that may be used in more specialised and demanding applications such as automotive paints and construction plastics [1–6]. As polymeric and composite materials are replacing metals in applications such as automotive manufacture, demand for these high performance types of pigments has increased. Two such high-performance pigments, a copper phthalocyanine and a quinacridone, have been selected for use in an impact-modified blend of a polycarbonate (PC) and poly(butylene terephthalate) (PBT). It was considered to be essential that the pigments were characterised before they were added to the polymer formulations. This paper focuses on some of the more relevant pigment characteristics that were thought to influence the final pigmented polymer product.

Pigmented polymer blends are complex in several ways. They possess compositional heterogeneity as well as different extents and types of interaction, as seen in preferential adsorp-

tion behaviour [3]. The inverse gas chromatographic technique provides a means of quantifying the overall effect of such interactions as well as a means of studying features arising from the more specific interactions.

With respect to PBT, Santos et al. have studied the surface characteristic by means of the IGC technique. In their work the specific component of the adsorption of polar probes was noted to be endothermic. The change in the entropy of the system was positive, an uncommon situation in the case of IGC studies. The results were interpreted in terms of cleavage of H-bonds in the PBT and the formation of H-bonds between the probe molecules and the polymer. The Lewis acidity constant and the Lewis basicity constant correlated well with analyses of the repeating unit and the end groups of the polymer [7].

In an extension of their work, Santos et al., used the IGC technique to study the interactions between pigments (particularly cobalt aluminate) in impact modified PC-PBT blends. The determined values of the various types of interaction allowed the authors to provide a rationale for an interpretation of the phase separation and the phase preferences that exist in the chosen polymer blend system. An attempt was made to explain observed changes that took place in the physical properties and in the chemical properties of the pigmented polymer blends in

* Corresponding author. Tel.: +44 113 343 2934; fax: +44 113 343 2947.
E-mail address: ccdjt@leeds.ac.uk (J.T. Guthrie).

terms of the data that were provided by the IGC evaluations [8].

Various other workers have considered the use of IGC in the study of pigmented polymer blends, with some emphasis being placed on colour development, gloss, rheological properties, adhesion and mechanical properties. Schreiber used IGC techniques in a study of pigmented, plasticized PVC systems, correlating IGC results with those concerning the rheological properties and the mechanical properties [9]. Lee et al., studied the significance of the acid–base properties of surface modified TiO₂ pigmentary particles and their influence on the dispersion qualities of the pigments when in polymeric matrixes [10]. Ziani et al., studied the dispersion stability of pigments in paint formulations and concluded that a correlation exists between the ease of dispersion and the acid–base interaction parameters, as determined by IGC [11]. Such findings support those made by Kunaver et al., in their IGC study of interactions in pigmented, high solids coatings formulations [12]. A summary of such work has been provided by Santos. However, whilst considering organic pigmented polymeric composites, Santos was mainly interested in interactions that take place between pigments and their polymeric matrix, as encountered in blend compositions [13].

The copper phthalocyanine pigment evaluated in this work was C.I. Pigment Blue 15:4. This is the flocculation-stabilised, β -phase form of the pigment. This pigment is bright, has a high tinctorial strength, has renowned durability and is very cost effective in use. There are two major methods of manufacturing copper phthalocyanine pigments. These methods are well described in the literature, as are the properties of the pigment [14–16].

The quinacridone pigment that was evaluated in this work was C.I. Pigment Red 122, a 2,9-dimethylquinacridone, a linear *trans*-quinacridone. It has a very clean, bluish shade of red. This quinacridone has excellent migration fastness and heat stability [17–25].

2. Experimental

There are many properties of interest in the practical application of pigments [26]. Such properties are dependent on the size, the shape and the surface characteristics of the pigment particles. Thus, the analyses used in this study of the pigments may be divided into two aspects: characterisation of the pigment geometry (e.g. particle size, shape, surface area) and characterisation of the surface chemistry. A selection of experimental techniques addressing both of these aspects has been used to study the two pigments of interest: C.I. Pigment Red 122 and C.I. Pigment Blue 15:4.

2.1. Materials

The copper phthalocyanine pigment studied was C.I. Pigment Blue 15:4 (Heliogen Blue FK4207, supplied by BASF, Stuttgart, Germany). This pigment was supplied in the form of a blue powder, and was used without further treatment. The structure of C.I. Pigment Blue 15:4 is shown in Fig. 1a.

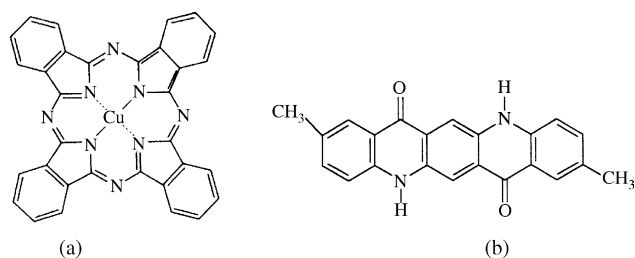


Fig. 1. Chemical structures of the pigments studied: (a) C.I. Pigment Blue 15:4 and (b) C.I. Pigment Red 122.

The quinacridone pigment studied was C.I. Pigment Red 122 (supplied by Bayer, Mijdrecht, The Netherlands). This pigment was supplied in the form of a magenta powder, and was used without further treatment. The chemical structure of C.I. Pigment Red 122 is shown in Fig. 1b.

For IGC studies, analytical grade probes were used without further purification. All were supplied by Sigma–Aldrich, Gillingham, Dorset, UK. The apolar probes used were: *n*-hexane, *n*-heptane, *n*-octane, *n*-nonane and *n*-decane. The polar probes used were: tetrahydrofuran (THF), acetone (Acet), dichloromethane (DCM), trichloromethane (TCM), ethyl acetate (EtAc) and diethyl ether (DEE). The carrier gas used was helium (>99.999% purity; supplied by BOC Gases, Guildford, UK). The non-interacting reference probe was methane (supplied by Phase Separations, Deeside, UK).

2.2. Scanning electron microscopy (SEM)

SEM evaluations were undertaken to assess the shapes of the pigment particles. Two methods were used to evaluate the shape and appearance of the pigment particles: as supplied for use, and as dispersed (i.e. with agglomerates and aggregates broken down to give the primary particles). These methods are referred to as the direct method and the dispersion method, respectively. A Jeol JSM-820 scanning experimental electron microscope was used for SEM evaluations.

2.2.1. Direct method of pigment evaluation

Small samples of pigments were mounted onto brass stubs, in order to evaluate them in a “natural” state (i.e. the way in which they are supplied to go into the polymer extrusion formulations). A Bio-Rad SEM Coating System was used to gold coat the samples, with a depth of gold of approximately 40 nm. For the C.I. Pigment Red 122 sample, an accelerating voltage of 5 kV was used, and a micrograph was recorded at a magnification of $\times 100$. For the C.I. Pigment Blue 15:4 sample, the accelerating voltage used was 10 kV and a micrograph was recorded at a magnification of $\times 1000$. The conditions were different for the two pigments due to their very different appearances when evaluated by SEM, as indicated by the different tendencies towards surface charge build up.

2.2.2. Dispersion method of pigment evaluation

The pigments were dispersed in distilled water with the aid of a non-ionic surfactant. The dispersions were then subjected to

ultrasonic mixing for 2–3 min to break down as many agglomerates as possible. The dispersed pigments were then dropped onto 0.025 μm (pore size) Whatman Anodiscs (inorganic membranes) and mounted. The samples were gold coated (the layer of gold being approximately 40 nm in depth) and examined by SEM. For the C.I. Pigment Red 122 sample an accelerating voltage of 20 kV was used, and micrographs were recorded at magnifications of $\times 8000$ and $\times 10\,000$. For the C.I. Pigment Blue 15:4 sample, an accelerating voltage of 20 kV was used. Micrographs were recorded at magnifications of $\times 5000$ and $\times 8000$.

2.3. Particle sizing

Particle sizing analyses were carried out to evaluate the mean particle size, and particle size distribution of the two pigments. Photo-correlation spectroscopy was the technique used. Particle sizing was carried out on dispersions of C.I. Pigment Red 122 and C.I. Pigment Blue 15:4. To create a dispersion, a small amount of pigment was wetted with Surfynol CT-121 (Air Products, Utrecht, The Netherlands), a non-ionic surfactant. The mixture was diluted with distilled water that contained a few drops of the surfactant, and stirred thoroughly. The dispersion was then sonicated in an ultrasonic bath for 2 min. Immediately after sonication, the dispersion was analysed in a Coulter Model N4MD sub-micron particle analyser. Immediate analysis was necessary to avoid the consequences of flocculation of the particles that might occur with time. The analysis parameters used were: temperature 20 °C, viscosity 0.977 mPa s, refractive index 1.333 and angle 90°.

2.4. BET surface analysis

BET surface analysis was carried out on C.I. Pigment Red 122 and C.I. Pigment Blue 15:4 samples. This was done using an Accelerated Surface Area and Porosimetry System (Micromeritics ASAP 2000). Standard procedures of sample preparation and measurement were followed.

An amount of pigment that was estimated to give a surface area of approximately 10 m² was transferred to the sample tube. The sample tube was connected to the degas port of the Micromeritics system. De-gassing of the sample was carried out at room temperature, under a vacuum to remove moisture and other contaminants. The de-gassing vacuum level was set to 66.5 Pa.

2.5. Inverse gas chromatographic (IGC) evaluation

The IGC technique provides a means of gaining information concerning the surface polarity of particulates and the acid–base nature of particulates. This information is important to this study. It provides a basis for determining the potential for chemical interaction between the pigment and its medium (the polymer matrix). The evaluation was carried out via studies of the interactions of the pigment with well-characterised organic probes. A column containing the material of interest was placed between the injector and detector of a gas chromatography unit. The

pigments were evaluated via the study of injections of volatile probes possessing known properties, which were carried through the column via an inert carrier gas. The retention time of each probe is related to the surface properties of the stationary phase. The theory and the technique are now quite well described in the literature [7,8,27,28].

2.5.1. Theory

The interaction between the pigment and the probe is quantified by the retention time for the particular probe. The retention time, t_r , is dependent upon the carrier gas flow rate that is used in the experiment. Thus, a net retention volume, V_n , is determined. V_n is defined by the equation:

$$V_n = (t_r - t_0)FJC.$$

Here, t_r and t_0 are the retention times of the probe and of a non-interacting probe (e.g. methane), respectively. F is the carrier gas flow rate, J is a correction factor used to correct for the compressibility of the carrier gas and C is a correction factor to allow for the vapour pressure of the water in the bubble flow meter at the measurement temperature. The terms J and C may be defined separately. Thus, for J ,

$$J = 1.5 \frac{(P_1/P_0)^2 - 1}{(P_1/P_0)^3 - 1}.$$

Here, P_1 and P_0 are the inlet pressure and outlet pressure of the carrier gas, respectively. For C , the relationship is:

$$C = 1 - \frac{P_{\text{H}_2\text{O}}}{P_0}.$$

Here, $P_{\text{H}_2\text{O}}$ is the vapour pressure of the water in the flow meter at the measurement temperature.

The net retention volume may be normalised, to give the specific retention volume, V_g , as

$$V_g = \frac{V_n}{m}.$$

Here, m is the mass of interacting material in the stationary phase.

The Fowkes approach is used to determine the free energy of adsorption and the dispersive component of the pigment surface tension. The approach is based on the work of adhesion of the probe on the pigment surface. The work of adhesion (W_a) between species interacting only via dispersive forces is given by the equation:

$$W_a = 2(\gamma_s^d \gamma_1^d)^{0.5}.$$

Here, γ_s^d and γ_1^d are the dispersive components of the surface energies of the pigment and of the probe, respectively.

The work of adhesion is related to the free energy of adsorption of the probe by the equation

$$-\Delta G_a^\circ = NaW_a + K'.$$

Here, N is the Avogadro's number, a the molecular surface area of the probe and K a constant.

Table 1
Values of $a(\gamma_1^d)^{0.5}$ for the selected *n*-alkane probes

Probe	$a (\times 10^{-10} \text{ m}^2)$	$\gamma_1^d (\text{mJ/m}^2)$	$a\sqrt{(\gamma_1^d)} (\text{m}^2(\text{mJ/m}^2)^{0.5})$
<i>n</i> -Hexane ^a	51.5	18.4	2.21×10^{-18}
<i>n</i> -Heptane ^a	57.0	20.3	2.57×10^{-18}
<i>n</i> -Octane ^a	62.8	21.3	2.90×10^{-18}
<i>n</i> -Nonane ^a	68.9	22.7	3.28×10^{-18}
<i>n</i> -Decane ^b	75	23.4	3.63×10^{-18}

^a [29].

^b [30].

The free energy of adsorption (ΔG_a) may also be defined in terms of the retention volume of the probes:

$$\Delta G_a = -RT \ln(V_n) + K.$$

T is the column temperature and K is a constant for a given column.

Consequently, the equations may be combined to give:

$$-\Delta G_a = RT \ln(V_n) = 2Na(\gamma_s^d)^{0.5}(\gamma_1^d)^{0.5} + K''$$

Thus, for a series of *n*-alkane probes, a plot of $RT \ln V_g$ against $a(\gamma_1^d)^{0.5}$ will give a slope of $2N(\gamma_s^d)^{0.5}$. Values of $a(\gamma_1^d)^{0.5}$ are found in the literature. The values used in this study are presented in Table 1.

If polar probes are used, specific interactions with the pigment surface are possible. Thus, there will be a specific component to the total surface free energy in addition to the dispersive component. The total free energy of adsorption, ΔG_a^{tot} , can then be defined as:

$$\Delta G_a^{\text{tot}} = \Delta G_a^d + \Delta G_a^s.$$

Here, ΔG_a^d and ΔG_a^s are the dispersive contribution and the specific contribution, respectively. The specific component of the free energy is determined from the *n*-alkane plot of $RT \ln V_g$ against $a(\gamma_1^d)^{0.5}$. The distance between the ordinate values of the polar probe datum point and the *n*-alkane reference line gives the specific component of the surface free energy.

An equation may be written for this procedure. Thus,

$$-\Delta G_a^s = RT \ln \left(\frac{V_n^{\text{tot}}}{V_{n,\text{ref}}^d} \right).$$

Table 2
Values of $a(\gamma_1^d)^{0.5}$, DN and AN* for the selected polar probes

Probe	$a (\times 10^{-10} \text{ m}^2)$	$\gamma_1^d (\text{mJ/m}^2)$	$a\sqrt{(\gamma_1^d)} (\text{m}^2(\text{mJ/m}^2)^{0.5})$	AN* (kJ/mol)	DN (kJ/mol)
Tetrahydrofuran (THF) ^a	45.0	22.5	2.13×10^{-18}	2.1	84.0
Dichloromethane (DCM) ^b	31.5	27.6	1.65×10^{-18}	16.4	0.0
Chloroform (TCM) ^b	44.0	25.9	2.24×10^{-18}	22.7	0.0
Diethyl ether (DEE) ^a	47.0	15.0	1.82×10^{-18}	5.9	80.6
Ethyl acetate (EA) ^a	48.0	19.6	2.13×10^{-18}	6.3	71.8
Acetone (Ace) ^a	42.5	16.5	1.73×10^{-18}	10.5	71.4

AN* and DN calculated from [32].

^a [29].

^b [31].

Here, V_n^{tot} and $V_{n,\text{ref}}^d$ are the retention volume for the polar probe and the retention volume for the *n*-alkanes' reference line, respectively.

Values of $a(\gamma_1^d)^{0.5}$ for the polar probes used in this study are presented in Table 2.

The adsorption of a polar probe onto the pigment surface leads to a change in the enthalpy of the system and the entropy of the system. These factors are related to the energy of adsorption by the equation,

$$\Delta G_a = \Delta H_a - T\Delta S_a.$$

Here, ΔH_a is the change in enthalpy, ΔS_a is the change in entropy and T is the column temperature. For each polar probe, ΔH_a and ΔS_a can be determined from a plot of $\Delta G_a/T$ against $1/T$.

The surface Lewis acidity and basicity constants, K_a and K_b , may be calculated from the equation,

$$-\Delta H_a = K_a DN + K_b AN^*.$$

Here, DN and AN* are Gutman's donor and modified acceptor numbers, respectively. Values of DN and AN* for the polar probes used in this study are given in Table 2.

K_a and K_b are obtained from a plot of $-\Delta H_a/AN^*$ versus DN/AN^* , with K_a as the slope and K_b as the intercept.

2.5.2. Column preparation [7,8]

Stainless steel columns of length 0.5 m and internal and external diameters of 4.4 and 6.4 mm, respectively, were selected. Each was formed into a smooth U-shape to fit the geometry of the instrument. Prior to use, the internal surfaces of the columns were cleaned. This was achieved by rinsing with a hot aqueous detergent solution ("Decon 90", 5%), followed by steeping in acetone, then washing with distilled water, and finally acetone. The columns were then allowed to dry in a vacuum oven at 100 °C.

2.5.3. Column packing preparation

It was necessary to use different support materials for the two pigments under study. Chromosorb W AW DCMS (Supelco), particle size 60–80 mesh was used for C.I. Pigment Blue 15:4. For C.I. Pigment Red 122, it was observed that the use of this particular column support gave rise to a much greater degree of column packing, resulting in a very high pressure drop across the

column. For this reason, glass beads (Supelco), with a diameter of 75 μm , were employed instead. The experimental procedures associated with sample preparation are described elsewhere [7,8].

2.5.4. Column assembly

Before each column was filled, it was weighed five times and an average mass calculated. The packing material was then introduced into the column using a funnel. Small additions were made to each end in turn, and the column tapped gently to facilitate better packing. When the column was filled to within 5 mm of the ends, the column was reweighed five times. Again, an average value was calculated. The mass of material in the column (and hence the mass of pigment) was then calculated by difference. Finally, the columns were “sealed” with small plugs of silanized glass wool (Phase Separations). To ensure that all volatiles had been removed from the columns, each was conditioned overnight before use. This was carried out under a helium flow rate of approximately 25 mL/min and at a temperature of 140 °C. This was to ensure the removal of any residual volatiles that would otherwise have affected the retention of the probes on the materials being studied.

2.5.5. Inverse gas chromatography procedure

A Fisons 8000 Series gas chromatograph with a flame ionisation detector was used to carry out the studies. The injector and detector temperatures were set to 150 and 180 °C, respectively. The oven temperature range selected was different for the two pigments. C.I. Pigment Blue 15:4 was studied between 100 and 140 °C, while C. I. Pigment Red 122 was studied between 80 and 120 °C. Both pigments were studied using columns with a level of pigment of 1.5% (w/w). Helium (99.999% purity) was used as the carrier gas, and the flow rate was varied via a needle valve pressure regulator [8]. The flow rate was measured using a bubble flow meter, equipped with a helium trap and a thermometer. Each flow rate was measured in triplicate, and an average value obtained. The inlet pressure was read from a pressure gauge, and the atmospheric pressure was obtained from the British Atmospheric Data Centre (www.badc.rl.ac.uk).

Methane (Phase Separations) was employed as a non-interacting reference probe. The non-polar and polar probes (Aldrich) selected for the studies were analytical grade and were

used without further purification. A small volume of each probe was kept in a sealed vial, enabling the vapour to be extracted and injected into the instrument. Typically, volumes of up to 1 μL of probe vapour were injected using a 1.0 μL Hamilton syringe. For the higher alkanes (*n*-nonane, *n*-decane) it was necessary to use much larger volumes (up to 30 μL) using a 50 μL Hamilton syringe. At least three elution profiles were obtained for each probe.

The retention times were calculated using the Condor and Young method [33]. This method determines the time to the mass centre of the peak (the time to 50% elution) where probes are observed to exhibit significant tailing. If there is little or no tailing, the mass centre is equivalent to the time at the peak maximum. Tangents were constructed on the steepest parts of the retention peak and extended to intersect the baseline. The intersection of the leading tangent gives time t_1 and the intersection of the tailing tangent gives time t_2 . The retention time is calculated using the equation:

$$t_r = \frac{t_1 + t_2}{2}.$$

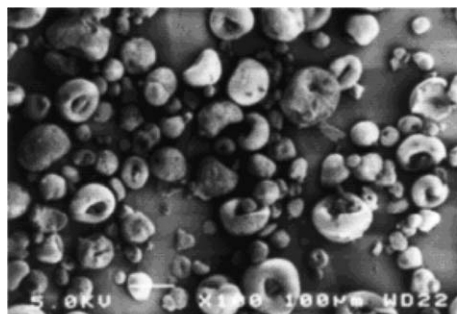
Three retention times were calculated for each probe, and a mean value obtained for use in further calculations.

3. Results and discussion

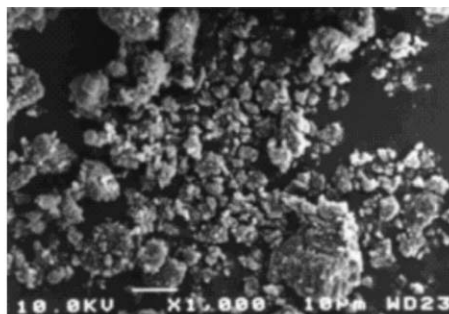
3.1. Scanning electron microscopic (SEM) evaluations

3.1.1. Direct method of SEM evaluation of the pigments

The micrographs of the two pigments in their supplied states are shown in Fig. 2. In Fig. 2a, 1 cm of the pictorial representation is equivalent to 125 μm of size dimension. In Fig. 2b, 1 cm of the pictorial representation is equivalent to 14 μm of size dimension. C.I. Pigment Red 122 appears as roughly spherical particles (of diameter 45–80 μm), with some larger ring-shaped particles (of a minimum diameter of 100 μm). This sample has been described as having undergone “classic doughnut spray drying”, with the spherical particles making the pigment easier to handle [34]. The C.I. Pigment Blue 15:4 sample studied has a very different appearance. The sample consists of uneven aggregates of particles, covering a wide range of sizes.



(a) C.I. Pigment Red 122



(b) C.I. Pigment Blue 15:4

Fig. 2. SEM micrographs of the pigments as supplied.

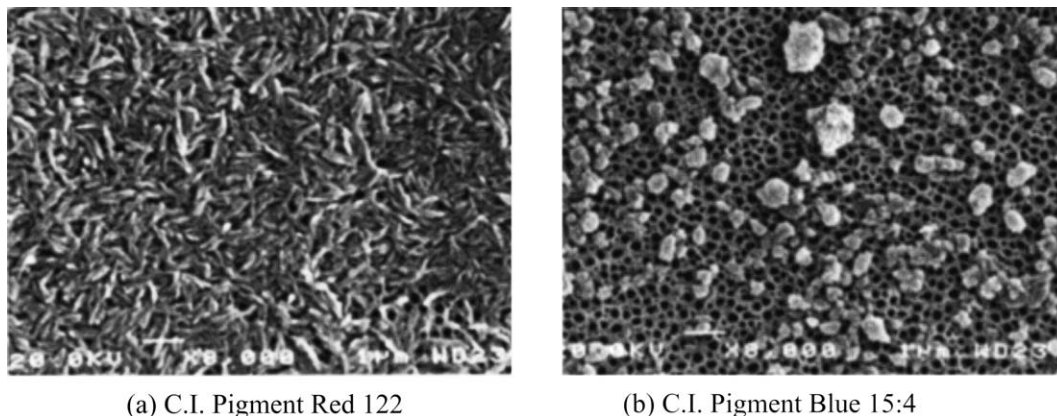


Fig. 3. SEM micrographs of the dispersed pigments.

3.1.2. Dispersion method of SEM evaluation of the pigments

The micrographs recorded for the dispersed pigment samples are shown in Fig. 3. In these micrographs, the scales are equivalent for the two images, and 1 cm of the pictorial representations is equivalent to $1.7\ \mu\text{m}$ of size dimension. The spherical species in the sample of C.I. Pigment Red 122 are now shown to have been broken down to release the primary pigment particles. These are acicular (needle-shaped), and seem to be of a regular size. However, it is difficult to determine accurately the dimensions of the individual particles. The dispersed particles of C.I. Pigment Blue 15:4 appear to have maintained their irregular shapes, but the range of sizes is reduced. The majority of the aggregates have a diameter of less than $1\ \mu\text{m}$.

3.2. Particle sizing

A unimodal analysis and a size distribution processor (SDP) analysis were carried out for each pigment. The data for the unimodal distributions that were obtained for C.I. Pigment Blue 15:4 and C.I. Pigment Red 122 are shown in Table 3.

These results indicate that the particles of C.I. Pigment Blue 15:4 are smaller than the particles of C.I. Pigment Red 122. There is, however, a broader distribution of the particle sizes in the sample of C.I. Pigment Blue 15:4 than in that of C.I. Pigment Red 122. These measurements are in agreement with the observations made from the SEM images.

The results from the SDP particle size analyses are shown in Table 4. These results confirm the observations made from the unimodal analyses, and prove that the distribution is truly unimodal. The sample of C.I. Pigment Blue 15:4 has a much wider range of particle sizes than is possessed by the sample of

C.I. Pigment Red 122. The particles of C.I. Pigment Red 122 are again shown to be larger than those of C.I. Pigment Blue 15:4.

3.3. BET surface analysis

Analyses were carried out to determine the BET surface area of a sample of each of the pigments. The surface area is an important application parameter as the surface contributes to the potential for interaction between the pigment and the polymer matrix in pigmented polymer blends. An isotherm was obtained for each sample using nitrogen molecules at a temperature of $-196\ ^\circ\text{C}$. The isotherms determined for the adsorption process and for the desorption process of nitrogen on the surfaces of C.I. Pigment Blue 15:4 and C.I. Pigment Red 122 are shown in Fig. 4. Each isotherm provides information regarding the monolayer capacity and the multi-layer adsorption characteristics of the pigment surface, together with information concerning interactions occurring between the pigment particles.

The first part of the isotherm (up to the relative pressure at which the isotherm starts to increase dramatically) corresponds to the adsorption of a monolayer of nitrogen molecules on the available pigment crystal surfaces. The BET equation was applied to the data in this part of the isotherm, to determine the monolayer capacity of the pigment, and to establish the nature of the adsorption, if any, in the second region of the isotherm.

This second region of the isotherm corresponds to “multi-layer adsorption” of nitrogen molecules on the pigment surface. The hysteresis loop in this region provides information concerning the energies of interaction that are associated with this behaviour. A hysteresis loop is formed if the nitrogen is able to “condense” in the pores between the pigment crystals, as differ-

Table 3
Data obtained from the unimodal particle size distribution analyses

	C.I. Pigment Red 122	C.I. Pigment Blue 15:4
Mean diameter (nm)	282	158
95% limits (nm)	266–297	151–164
Standard deviation (nm)	“Narrow”	58

Table 4
Data obtained from the SDP particle size distribution analyses

Size (nm)	Amount (%)	
	C.I. Pigment Red 122	C.I. Pigment Blue 15:4
100	0	14
178	1	80
316	99	6

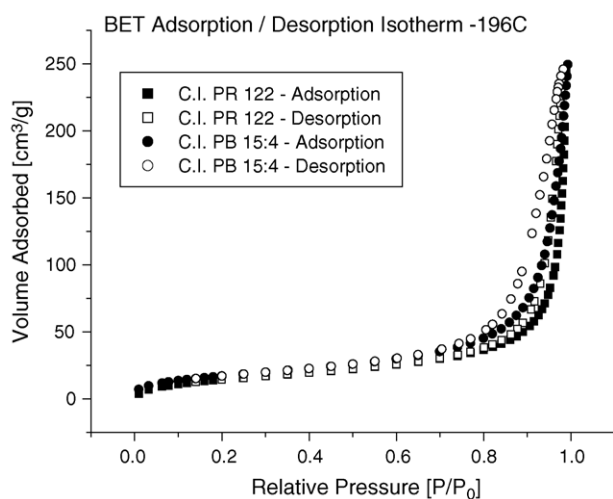


Fig. 4. The BET adsorption/desorption isotherms of C.I. Pigment Blue 15:4 and C.I. Pigment Red 122.

ent levels of interaction, with associated energies, take place for the adsorption and the desorption processes.

The isotherms in Fig. 4 indicate that both pigments are quite strongly coherent as there is little low-pressure hysteresis. This suggests that the pigment crystals are sufficiently well packed to prevent significant amounts of nitrogen entering into any void spaces. C.I. Pigment Blue 15:4 gives more high pressure hysteresis than that provided by C.I. Pigment Red 122. This implies that the phthalocyanine pigment (C.I. Pigment Blue 15:4) has better ordered character within the sample than does the quinacridone (C.I. Pigment Red 122).

The computer software associated with the ASAP 2000 System carries out the calculations that are needed to determine the BET surface area of the pigment sample. The results obtained are summarised in Table 5.

As these results show, the C.I. Pigment Blue 15:4 sample has a slightly larger surface area than that possessed by the C.I. Pigment Red 122 sample.

3.4. Inverse gas chromatography studies

In preliminary experiments, the influence of pigment loading, on the support material as a “concentration” series, was evaluated to ensure that, in the investigations described here, complete coverage of the support material was a reality, within experimental error. In this way, it was possible to ensure that the observations made in experiments were not influenced by the amount of coverage and that no “naked” zones of support material were present to cause complications in the behaviour observed [35].

Table 5
The results of the BET analyses

	C.I. Pigment Blue 15:4	C.I. Pigment Red 122
BET surface area (m ² /g)	65.18 ± 0.25	56.97 ± 0.15
Correlation coefficient	1.00	1.00

3.4.1. Evaluation of C.I. Pigment Red 122 and of C.I. Pigment Blue 15.4

Determination of the dispersive component of the surface free energy of C.I. Pigment Red 122 and of C.I. Pigment Blue 15.4. The Fowkes approach was used to determine the dispersive component of the surface free energy over a range of temperatures. For each temperature of study, the calculated values of $RT \ln V_g$ were plotted against $a(\gamma_1^d)^{0.5}$. These details are shown in Fig. 5a–e for C.I. Pigment Red 122 and Fig. 8a–e for C.I. Pigment Blue 15.4. Data obtained from studies of polar probes are included in these graphs. These data are discussed later in this paper.

Although the Fowkes data analytical approach has a relatively simple background, the results can be relatively easily rationalised within the objectives of the study undertaken. The data so derived are interpreted on the basis of the Fowkes model and used within the limitations of the model, bearing in mind the potential complexity of the systems being investigated. Thus, a good correlation coefficient was obtained from each of the linear fits, denoted as R^2 in each of the plots. The slope of the linear fit, obtained for each *n*-alkane plot, gives the dispersive component of the surface free energy, γ_s^d , at that temperature. To determine the relationship between these two parameters, the values are shown in Table 6 for C.I. Pigment Red 122.

Table 6 shows that the dispersive component of the surface free energy decreases as the temperature increases. This follows a logical trend as the weaker the dispersive interaction, the easier it would be to remove the molecules from the surface.

However, there was significant variation in the values of the dispersive component of the surface energy as the temperature increased. Further experimental work is necessary to understand the reason for such variation, although owing to the high quality of experimental consistency, it is felt that the variation is indicative of the changing nature of the pigment (steric, chemical) as a function of temperature.

Determination of the specific component of the surface free energy of C.I. Pigment Red 122 and of C.I. Pigment Blue 15.4. The behaviour of a range of polar probes was used to determine the specific component of the surface free energy. The acidic probes that were studied were trichloromethane (TCM) and dichloromethane (DCM). A single basic probe, tetrahydrofuran (THF), was studied in the same way. The amphoteric probes included acetone, diethyl ether and ethyl acetate.

As for the *n*-alkanes, values of $RT \ln V_g$ were calculated for each of the polar probes that were studied. Plots of these values of $RT \ln V_g$ against $a(\gamma_1^d)^{0.5}$ are included in Fig. 5a–e, at the relevant temperature. The specific component of the surface free energy,

Table 6
Values of γ_s^d with increasing temperature for C.I. Pigment Red 122

Temperature (°C)	γ_s^d (mJ/m ²)
80	49.72
90	46.72
100	42.62
110	34.09
120	32.46

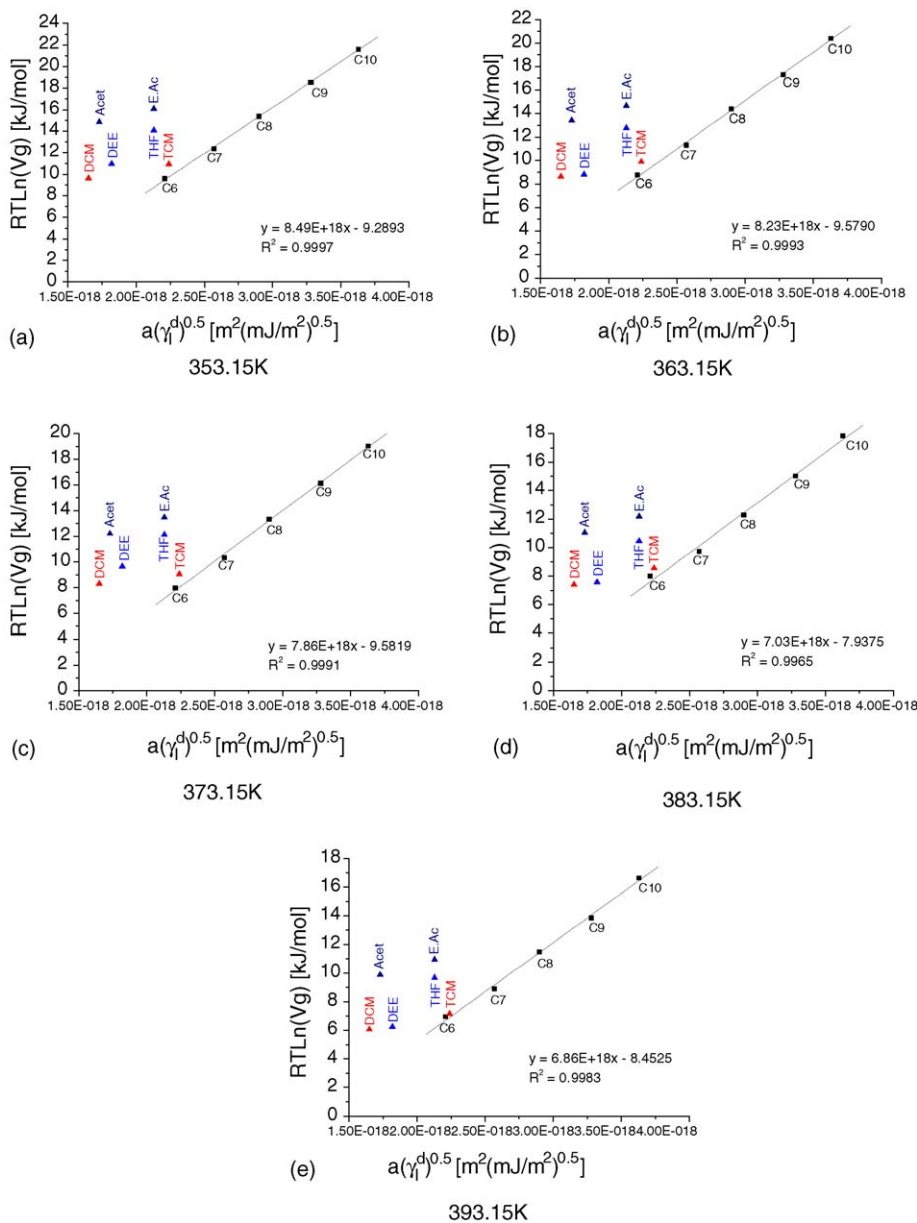


Fig. 5. A plot of $RT \ln(V_g)$ vs. $a(\gamma_1^d)^{0.5}$ for n -alkanes and polar probes, on C.I. Pigment Red 122.

$-\Delta G_a^s$, is calculated using the difference between the calculated value of $RT \ln V_g$ and that which was derived using the equation of the linear fit of the n -alkane reference line.

By plotting the values of $-\Delta G_a^s/T$ against $1/T$, the enthalpy and entropy of adsorption was determined for each polar probe. It should be recalled that ΔG_a , ΔH_a and ΔS_a relate to the change in the thermodynamic term respectively on adsorption. The equation $\Delta G_a = \Delta H_a - T\Delta S_a$ was applied, so that ΔH_a was determined from the slope and ΔS_a was determined from the intercept of the linear regression applied. These data representations are shown in Fig. 6. The values of the enthalpy of adsorption and of the entropy of adsorption for polar probes are given in Table 7.

The value of ΔH_a indicates the strength of the interaction between the probe and the surface of the pigment.

Thus, the strength of interaction increases in the order: TCM < DCM < THF < DEE < EA < AC. This order suggests that the pigment has an amphoteric nature. However, it does not take into account the relative strengths of the basic probes and of the

Table 7

Values of the enthalpy and entropy of adsorption for the polar probes

Probe	ΔH_a (kJ/mol)	ΔS_a (kJ/mol)
THF	22.85	0.0495
Chloroform	8.88	0.0215
DCM	20.33	0.0433
Diethyl ether	25.50	0.0592
Ethyl acetate	30.65	0.0660
Acetone	37.63	0.0796

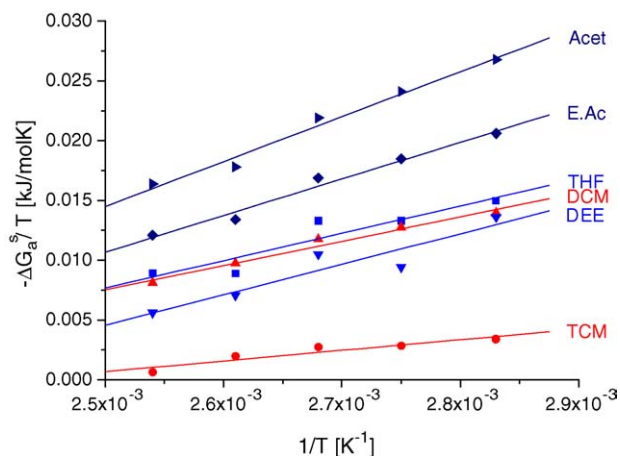


Fig. 6. Determination of the specific component of the enthalpy of adsorption and the entropy of adsorption for each of the polar probes on C.I. Pigment Red 122.

acidic probe molecules (i.e. THF is a much stronger base than DCM is an acid). Calculation of the values of K_a and K_b allows the determination of the Lewis acidity and the determination of the Lewis basicity of the pigment surface, respectively.

K_a and K_b are obtained from a plot of $-\Delta H_a/AN^*$ against DN/AN^* , with K_a as the slope and K_b as the intercept. This plot is shown in Fig. 7. From the linear regression of the data, K_a had a value of 0.2462, and K_b a value of 1.2664. Thus, it can be suggested that C.I. Pigment Red 122 is predominantly basic in nature. It should be recalled that the acronyms AN^* and DN relate to the acceptor number and donor number of the molecule in question. The data show a good level of consistency across the range of values of the ratio DN/AN^* for the series of probe molecules.

For C.I. Pigment Blue 15.4, values of $RT \ln V_g$ were calculated for each polar probe studied. Plots of these values against $a(\gamma_1^d)^{0.5}$ are included in Fig. 8a–e, at the relevant temperature. The values of $RT \ln V_g$ were calculated using an average value of t_r , which was determined from three experimental runs. However, as shown in Fig. 8 these values of $RT \ln V_g$ are accompanied

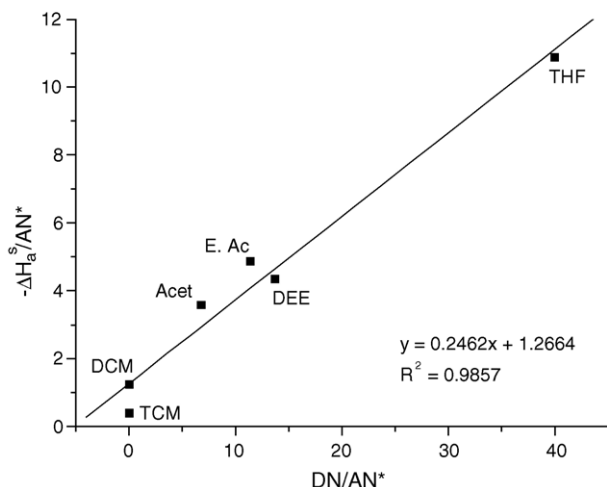


Fig. 7. Determination of K_a and K_b for C.I. Pigment Red 122.

by relatively large standard deviations (particularly for the acidic probes). These sets of experiments were repeated several times, but the spread of values was always found to exist. Thus, values of $-\Delta G_a^s$, the specific component of the surface free energy, could not be calculated with any degree of confidence.

These results suggest that C.I. Pigment Blue acts primarily through apolar forces. Very good correlation coefficients were obtained for the *n*-alkane probes, and the retention times for the polar probes were all very low (under 2 min). This observation is indicative of there being very little specific interaction between the probe and the pigment surface.

3.5. Postulated pigment–polymer interactions

As stated previously, the pigments under evaluation were to be incorporated into an impact modified Xenoy (PC-PBT) polymer blend. Santos and co-workers studied the major components of this blend by IGC [7,8]. The more pertinent results relevant to the study are given in Table 8, together with the results obtained for the pigments of interest to the current study. For the pigments C.I. Pigment Red 122 and C.I. Pigment Blue 15.4, the values of γ_s^d were observed to be temperature dependent, as indicated in Table 8 (by footnote b). The range for Pigment Red 122 was from 50 mJ/m² at 80 °C to 32 mJ/m² at 120 °C. For C.I. Pigment Blue 15.4, the values ranged from 72 mJ/m² at 100 °C to 48 mJ/m² at 130 °C. In both cases, there is reasonable linearity in the relationship with temperature, although greater scatter was observed in the case of the C.I. Pigment Blue 15.4. The lower values for γ_s^d that were observed for C.I. Pigment Red 122 could arise from the strong specific interactions between the molecules in the crystal lattice of the C.I. Pigment Red 122. These interactions cause the pigment to possess high stability features that one would not normally expect of a pigment of such a low molar mass (312 g/mol). These strong interactions concern the strong intramolecular hydrogen bonding that exists between the –CO groups and the NH groups of the pigment. These hydrogen bonds run through the lattice [17,18]. The findings in this present study complement the work described by Santos et al. [7,8]. It was determined [8] that the PBT would interact preferentially with itself, due to its relatively strong Lewis base character and Lewis acid functionalities. However, the strong Lewis basic sites can interact with the weaker Lewis acidic sites of the PC. Similarly, the Lewis acidic sites can interact with the Lewis basic sites of the PC. The impact modifier (IM) in the blend preferentially interacts with the PC rather than the PBT due to strong

Table 8

Surface characteristics of the major blend components, as determined by IGC

Component	γ_s^d (mJ/m ²)	K_a	K_b
PC ^a	33.3 ± 2.8	0.09	0.48
PBT ^a	42.3 ± 1.5	0.49	0.96
IM ^a	37.7 ± 1.6	0.10	1.14
C.I. Pigment Red 122	50–32 ^b	0.25	1.27
C.I. Pigment Blue 15:4	72–48 ^b	ND	ND

ND: not determined.

^a [23].

^b Temperature dependent values.

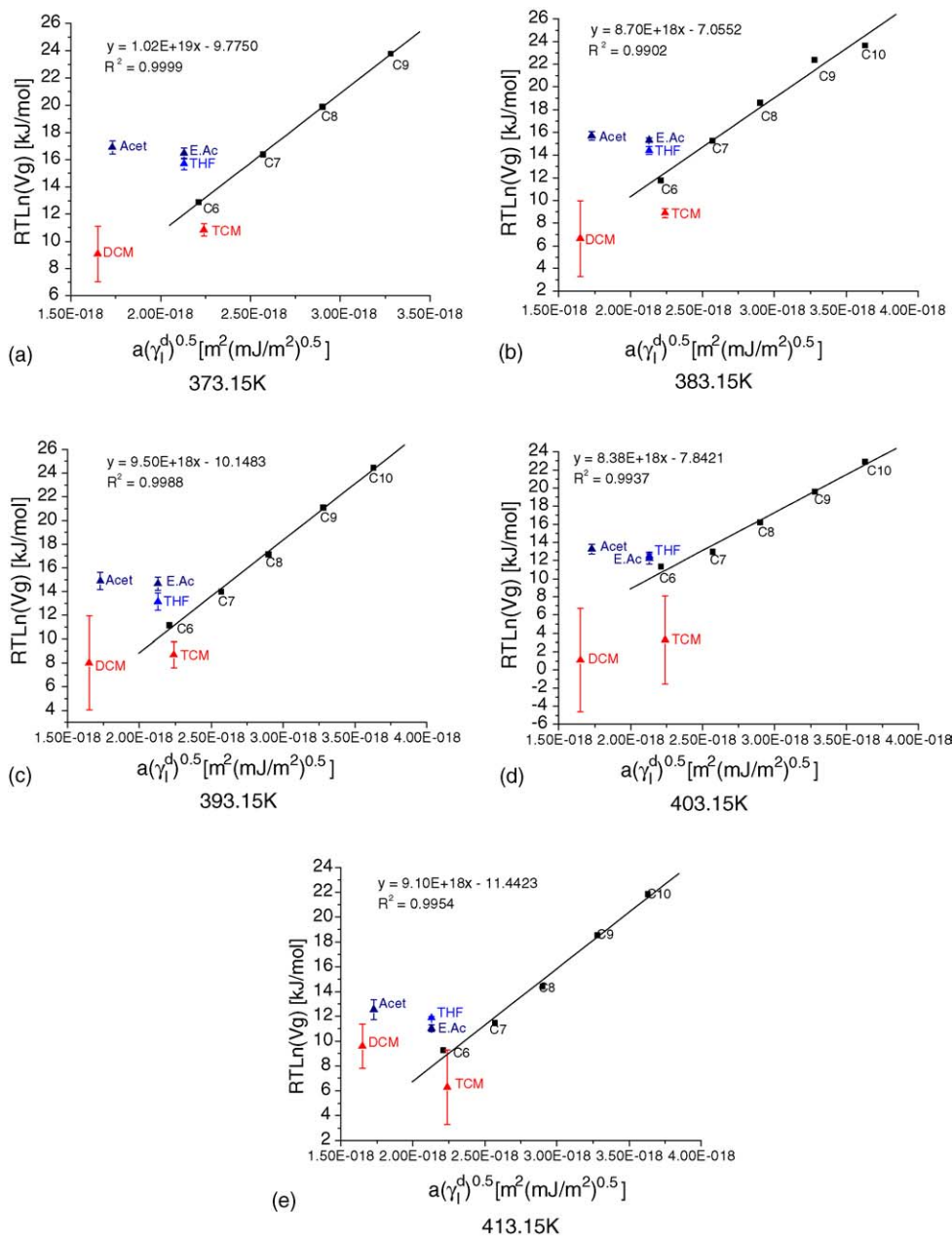


Fig. 8. A plot of $RT \ln(V_g)$ vs. $a(\gamma_1^d)^{0.5}$ for *n*-alkanes and polar probes, on C.I. Pigment Blue 15:4.

base–base repulsion between the PBT and itself. Being weakly Lewis acidic, the (IM) interacts primarily through its basic sites.

Considering the pigments studied, it appears that C.I. Pigment Red 122 is closest in its surface characteristics to the surface characteristics of the impact modifier. This pigment is amphoteric, though predominantly Lewis basic. Thus, the pigment will interact in a similar manner in which the impact modifier behaves and will preferentially interact with the PC component of the PC-PBT-IM blend. However, C.I. Pigment Red 122 has more Lewis acidic character than is possessed by the impact modifier. Thus, it may be possible for some interaction to take place between C.I. Pigment Red 122 and the Lewis basic sites of the PBT. It was not possible to determine values of K_a or K_b for C.I. Pigment

Blue 15:4 as this pigment appeared to interact primarily through apolar forces. Thus, the location of this pigment in the blend is determined more by the value of the dispersive component of the surface free energy, γ_s^d . Comparing the values in Table 8, it appears that the greatest interaction occurs between the pigment and the PBT. However, since all components have some capacity for apolar interaction, the pigment could be located elsewhere in the blend.

4. Conclusions

From the evaluations of the pigments that were carried out, a number of conclusions may be drawn:

- (1) C.I. Pigment Red 122 appears to be easier to disperse in polymer blends than is C.I. Pigment Blue 15:4. This finding has relevance to the colour of the polymer that is achievable through the pigment dispersion process and to other effects such as secondary migration phenomena and effects of the pigment, even when present in small amounts, on process properties and general physical properties.
- (2) Of the two pigment samples studied, C.I. Pigment Blue 15:4 has smaller particles and a wider particle size distribution than that possessed by C.I. Pigment Red 122. This suggests that the C.I. Pigment Red 122 will have superior fastness properties in terms of light-fastness, heat fastness and migration fastness. This point is of relevant to the maintenance of colour integrity of the blend during service.
- (3) C.I. Pigment Red 122 appears to be amphoteric, and predominantly Lewis basic in nature. This means that the pigment will have the ability to interact with species of a Lewis acidic nature or of a Lewis basic nature. Thus, its easier dispersibility and greater migration tendencies can be rationalised.
- (4) C.I. Pigment Blue 15:4 appears to act primarily through apolar forces and thus will have limited interaction with species of a Lewis acidic nature or Lewis basic nature. This point has relevance to the potentially reduced mechanical properties of the resultant pigmented polymer blends as seen in such events as crack propagation and the lesser resistance of such composites to surface attack.

Although these observations have been made, further studies of the final pigmented polymer system are needed to be undertaken to establish the relevance of these interpretations. This work is in hand.

Acknowledgement

The authors would like to acknowledge the assistance and financial support given by GE Plastics (Europe), Bergen op Zoom, The Netherlands, throughout this study.

References

- [1] Z. Hao, A. Iqbal, *Chem. Soc. Rev.* 26 (1997) 203.
- [2] M.J. Smith, *J. Oil Colour Chem. Assoc.* 57 (1974) 36.
- [3] J.T. Guthrie, L. Lin, *Physical-Chemical Aspects of Pigment Applications*, Oil & Colour Chemists Association, Wembley, 1994, pp. 21, 22.
- [4] R.B. McKay, *Spec. Publ. R. Soc. Chem.* 133 (1993) 107.
- [5] P. Günthert, P. Hauser, V. Radtke, *Rev. Progr. Coloration* 19 (1989) 41.
- [6] Kirk-Othmer, *Encyclopaedia of Chemical, Technology*, vol. 18, fourth ed., Wiley, New York, 1996, p. 1044.
- [7] J.M.R.C.A. Santos, K. Fagelman, J.T. Guthrie, *J. Chromatogr. A* 969 (2002) 111.
- [8] J.M.R.C.A. Santos, K. Fagelman, J.T. Guthrie, *J. Chromatogr. A* 969 (2002) 119.
- [9] H.P. Schreiber, in: G. Akozali (Ed.), *The Interfacial Interactions of Polymeric Composites*, Kluwer, Dordrecht, 1993, pp. 21–59.
- [10] Y.J. Lee, I. Manas-Zloczower, D.L. Feke, *Powder Technol.* 73 (1992) 139.
- [11] A. Ziani, R. Xu, H.P. Schreiber, T. Kobayashi, *J. Coat. Technol.* 71 (893) (1999) 53.
- [12] M. Kunaver, M.K. Gunde, M. Mozetic, A. Hrovat, *Dyes Pigments* 57 (2003) 235.
- [13] J.M.R.C.A. Santos, Ph.D. Thesis, University of Leeds, Leeds.
- [14] S.A. Faterpeker, *Paintindia* 39 (1989) 11.
- [15] W. Herbst, K. Hunger, *Industrial Organic Pigments: Production, Properties, Applications*, second revised ed., VCH, Weinheim, 1997, pp. 426–433.
- [16] P. Gregory, *J. Porphyrins Phthalocyanines* 4 (2000) 432.
- [17] W. Herbst, K. Hunger, *Industrial Organic Pigments: Production, Properties, Applications*, second revised ed., VCH, Weinheim, 1997, p. 454.
- [18] D.S. Filho, C.M.F. Oliveira, *J. Mater. Sci.* 27 (1992) 5101.
- [19] W. Herbst, K. Hunger, *Industrial Organic Pigments: Production, Properties, Applications*, second revised ed., VCH, Weinheim, 1997, pp. 455–459.
- [20] R.M. Christie, *Pigments Structures and Synthetic Procedures*, Oil & Colour Chemists Association, Wembley, 2003, p. 23.
- [21] G. Lincke, *J. Mater. Sci.* 32 (1997) 6447.
- [22] G.D. Potts, W. Jones, J.F. Bullock, S.J. Andrews, S.J. Maginn, *J. Chem. Soc., Chem. Commun.* (1994) 2565.
- [23] G. Lincke, *Dyes Pigments* 52 (2002) 169.
- [24] G. Lincke, *Dyes Pigments* 44 (2000) 101.
- [25] W. Herbst, K. Hunger, *Industrial Organic Pigments: Production, Properties, Applications*, second revised ed., VCH, Weinheim, 1997, p. 469.
- [26] R. Sappok, B. Honigmann, *Characterisation of Powder Surfaces*, Academic Press, London, 1976, p. 237.
- [27] R.J.E. English, Ph.D. Thesis, University of Leeds, Leeds, 1995.
- [28] A.J. Beaumont, Ph.D. Thesis, University of Leeds, Leeds, 1996.
- [29] J. Schultz, L. Lavielle, *Inverse Gas Chromatography Characterization of Polymers and Other Materials*, American Chemical Society, Washington, DC, 1989, p. 194.
- [30] D.P. Kamdem, S.K. Bose, P. Luner, *Langmuir* 9 (1993) 3039.
- [31] H. Chtourou, B. Riedl, B.V. Kokta, *J. Adhesion Sci. Technol.* 9 (1995) 551.
- [32] U. Panzer, H.P. Schreiber, *Macromolecules* 25 (1992) 3633.
- [33] J.R. Conder, C.L. Young, *Physicochemical Measurement by Gas Chromatography*, Wiley, Chichester, 1979, pp. 82, 83.
- [34] A. Kazlaucinas, personal communication, University of Leeds, Woodhouse Lane, Leeds LS2 9JT, UK.
- [35] K. Fagelman, Ph.D. Thesis, University of Leeds, Leeds, 2003.